THE JOURNAL OF BIOLOGICAL CHEMISTRY
Vol. 278, No. 49, Issue of December 5, pp. 48991–48996, 2003

Printed in U.S.A.

Solution Structure of the Dimeric Zinc Binding Domain of the Chaperone ClpX*

Received for publication, July 18, 2003, and in revised form, September 29, 2003
Published, JBC Papers in Press, October 1, 2003, DOI 10.1074/jbc.M307826200

Logan W. Donaldson‡§, Urszula Wojtyra¶, and Walid A. Houry¶

From the ‡Department of Biology, York University, Toronto, Ontario M3J 1P3, Canada and the ¶Medical Sciences Building, Department of Biochemistry, University of Toronto, Toronto, Ontario M5S 1A8, Canada

ClpX (423 amino acids), a member of the Clp/Hsp100 family of molecular chaperones and the protease, ClpP, comprise a multimeric complex supporting targeted protein degradation in *Escherichia coli*. The ClpX sequence consists of an NH_2-terminal zinc binding domain (ZBD) and a COOH-terminal ATPase domain. Earlier, we have demonstrated that the zinc binding domain forms a constitutive dimer that is essential for the degradation of some ClpX substrates such as λO and MuA but is not required for the degradation of other substrates such as green fluorescent protein-SsrA. In this report, we present the NMR solution structure of the zinc binding domain dimer. The monomer fold reveals that ZBD is a member of the treble clef zinc finger family, a motif known to facilitate protein-ligand, protein-DNA, and protein-protein interactions. However, the dimeric ZBD structure is not related to any protein structure in the Protein Data Bank. A trimer-of-dimers model of ZBD is presented, which might reflect the closed state of the ClpX hexamer.

Molecular chaperones and proteases are part of an essential quality control machinery in the cell, which ensures the conformational integrity of proteins under conditions of normal growth as well as under stress (1). In *Escherichia coli*, the chaperone ClpX, a member of the Hsp100 family (2–4), associates with the serine protease ClpP (5) to form a cylindrical structure that is similar to the 26 S proteasome (6, 7). Hexameric ClpX binds on one or both ends of tetradecameric ClpP (8). Specific biological processes mediated by ClpX include remodeling of bacteriophage MuA-DNA transposase complexes (9, 10), degradation of the λO replication protein (11), degradation of the UmuD′ subunit of error-prone DNA polymerase (12), and removal of LexA repressor protein fragments after RecA processing (13). Using an inactive ClpP mutant as a trap for native *E. coli* substrates, Flynn *et al.* (14) defined five classes of recognition sequences that are bound by ClpX. A more general class of substrates are directed to ClpXP via an SsrA tag (15–17), which is typically placed by a tmRNA at the COOH terminus of nascent chains stalled on the ribosomes. Additional specificity and regulation are provided by the accessory factors SspB (18, 19) and RssB (20), which promote interactions between ClpX and specific substrates.

ClpX sequence consists of an NH_2-terminal zinc binding domain (ZBD)[1] followed by one AAA ATPase domain (21–23). AAA domains are characterized by specific sequence motifs such as the Walker A and Walker B motifs (21). ClpX binds and, subsequently, unfolds and translocates substrate proteins into the ClpP chamber in an ATP-dependent manner. Other Clp/Hsp100 chaperones in *E. coli* include ClpA and ClpB. Both ClpA and ClpB have an NH_2-terminal domain followed by two AAA domains. ClpA also binds as a hexamer to ClpP oligomer, while ClpB does not seem to associate with any proteases. The N-domain of ClpA has been shown to be important for substrate binding (24) as well as for the binding of the cofactor ClpS (25). The ClpB N-domain has also been shown to be important for substrate binding (26), but no cofactor is yet known for ClpB. Despite the vast range of experimental techniques employed to study the mechanism of function of ClpXP and related systems, including electron microscopy (27), fluorescence-based methods (28, 29), molecular modeling (30), and others, very little insight has been gained regarding the ATP-dependent conformational changes that these molecular systems undergo during their functional cycle.

In an earlier paper (31), we had shown that the NH_2-terminal domain of ClpX is a C4-type ZBD involved in substrate and cofactor recognition. ZBD was shown to form a very stable dimer that is essential for promoting the degradation of some typical ClpXP substrates such as λO and MuA, but not green fluorescent protein-SsrA. Additional studies have shown that ZBD contains an essential binding site for the λO substrate and for the cofactor SspB. Removal of ZBD from the ClpX sequence renders the ATPase activity of ClpX largely insensitive to the presence of ClpP, substrates, or SspB cofactor. All these results indicate that ZBD plays an essential role in the ClpX mechanism of function and that ATP binding and/or hydrolysis drives a conformational change in ClpX involving ZBD.

As a subsequent step toward further characterizing the role of ZBD in the ClpX function, we have determined the solution structure of the ZBD homodimer using NMR methods. Although the structure of the monomeric subunit is well represented in the Protein Data Bank, the structure of the ZBD dimer is unique. The overall shape and internal symmetry observed for the ZBD dimer led us to create a trimer-of-dimers

* This work was supported by a grant from the National Sciences and Engineering Research Council (to L. W. D.) and by a grant from the Canadian Institutes for Health Research (to W. A. H.). The costs of publication of this article were defrayed in part by the payment of page charges. This article must therefore be hereby marked "*advertisement*" in accordance with 18 U.S.C. Section 1734 solely to indicate this fact.

The atomic coordinates and structure factors (code 1OVX) have been deposited in the Protein Data Bank, Research Collaboratory for Structural Bioinformatics, Rutgers University, New Brunswick, NJ (http://www.rcsb.org/).

§ To whom correspondence should be addressed: Dept. of Biology, York University, 4700 Keele St. West, 049 Farquharson, Toronto, Ontario M3J 1P3, Canada. Tel.: 416-736-2100 (ext. 22823); Fax: 416-736-5698; E-mail: logand@yorku.ca.

[1] The abbreviations used are: ZBD, zinc binding domain; AAA, ATPases associated with a variety of cellular activities; HSQC, heteronuclear single quantum coherence; NOESY, nuclear overhauser effect spectroscopy; r.m.s.d., root mean square deviation; TOCSY, total correlated spectroscopy.

model with a ring-like structure that complements the topology of the ClpX ATPase domain.

EXPERIMENTAL PROCEDURES

Protein Expression and Purification—Standard molecular biology techniques were used to construct a gene fragment encoding an amino-terminal Gly-His_6 tag followed by residues 1–60 of *E. coli* ClpX (residue number according to Swiss-Prot) that encompass the zinc binding domain. This fragment, flanked by NcoI and BamHI restriction sites, was inserted into pET28b (Novagen) for expression in *E. coli* BL21(DE3). A 2 L culture was incubated in a BioFlo 110 fermentor (New Brunswick Scientific) with [^{15}N]ammonium chloride and [^{13}C]glucose as the sole nitrogen and carbon sources following a published fermentation protocol (32). Divalent zinc was present as a trace mineral during the fermentation. Purification of ZBD was achieved by nickel affinity chromatography (Qiagen) and S-100 gel filtration (Amersham Biosciences).

Gel Filtration and Protein Cross-linking—Size exclusion chromatography was performed using a Superdex 200 HR 10/30 (Amersham Biosciences) column attached to an AKTA FPLC system (Amersham Biosciences). The column was equilibrated with 25 mM Tris-HCl, pH 8, 150 mM NaCl, and 1 mM dithiothreitol. Molecular mass standards (Sigma) used were: thryoglobulin (669 kDa), apoferritin (443 kDa), β-amylase (200 kDa), alcohol dehydrogenase (150 kDa), bovine serum albumin (66 kDa), carbonic anhydrase (21 kDa), and cytochrome *c* (12.4 kDa). All runs were performed at 4 °C, and the absorbance was monitored at 280 nm. For cross-linking, glutaraldehyde was added to a final concentration of 0.05% to a 30 μM solution of ZBD in 25 mM Hepes, pH 7.9, 150 mM NaCl, 100 μM $ZnCl_2$, and 1 mM dithiothreitol. Cross-linking was allowed to proceed for 15 min. The reaction was stopped by the addition of 0.5 M Tris-HCl, pH 8.0.

Circular Dichroism Spectra—CD spectra were obtained using an AVIV circular dichroism spectrometer model 62ADS equipped with a temperature controlled sample holder. The average of three spectra is reported, where each spectrum was collected by averaging the signal at every 1 nm for 1 s. Protein samples were measured in a 1-mm path length cuvette at a concentration of 30 μM.

NMR Spectroscopy—Samples for NMR spectroscopy contained 0.6–1.2 mM ZBD monomer in 10% D_2O, 20 mM sodium phosphate, pH 7.6, 150 mM NaCl, and 0.02% sodium azide. Backbone and side chain assignments were obtained using a combination of ^{15}N-HSQC, ^{13}C-HSQC, HNCO, HNCACB, H(CCO)NH-TOCSY, C(CO)NH-TOCSY, and (Hβ)Cβ(CγCδ)Hδ/Hε spectra recorded on 500 MHz Varian Inova and 600 MHz Bruker Avance NMR spectrometers at 30 °C. Data were processed and interpreted using NMRPipe (33) and NMRView (34) software. Intramolecular distance restraints were obtained from a three-dimensional simultaneous ^{13}C,^{15}N-edited NOESY with a 100 ms mixing time. Intermolecular distance restraints were obtained from a three-dimensional ^{12}C-filtered, ^{13}C-edited NOESY spectrum (35) using a hybrid ZBD dimer sample composed of ^{12}C, ^{14}N and ^{13}C, ^{15}N monomers dissolved in 99% D_2O. This hybrid sample was prepared by mixing equimolar quantities of unlabeled and isotopically labeled ZBD in the presence of 6 M guanidinium hydrochloride followed by rapid dilution into a 40-fold excess of NMR sample buffer to induce folding.

Structure Calculations and Model Building—Backbone dihedral angles were predicted from chemical shift information using the TALOS method (36). One Zn(II) ion was coordinated tetrahedrally to Cys^{14}, Cys^{17}, Cys^{36}, and Cys^{39} by a combination of bond and angle constraints. Initial structures from NOE and dihedral angle restraints were calculated using a modified ARIA 1.2 protocol (37) for dimeric proteins. Ramachandran data base and radius of gyration potentials were included during the calculation of the final ensemble with the XPLOR-NIH software package (38). The ZBD trimer-of-dimers model was created with Swiss PDB-Viewer (39). The figures were made with MOLMOL (40), Molscript (41), PyMOL (pymol.sourceforge.net/), and Raster3D (42). Coordinates have been deposited in the Protein Data Bank under accession code 1OVX. Chemical shift assignments have been deposited in the BioMagResBank under accession code 5665.

TABLE I
Statistics for the ensemble of structures calculated for the dimeric ZBD of ClpX

Ensemble of the top 25 structures out of 500 calculated with low energy and good geometry.

Distance restraints:	
Intramolecular, unambiguous	
Intraresidue	216
Sequential ($i - j = 1$)	143
Medium range ($2 \leq i - j \leq 4$)	56
Long range ($4 < i - j$)	60
Hydrogen bonds (HN–O, N–O)	12
Intramolecular, ambiguous	90
Intermolecular	47
Dihedral angle restraints:	
ϕ/ψ pairs	30
Pairwise r.m.s.d.	
All residues[a]	
Backbone atoms	0.94 ± 0.35
All heavy atoms	1.61 ± 0.35
Ordered regions[b]	
Backbone atoms	0.66 ± 0.27
All heavy atoms	1.27 ± 0.27

[a] r.m.s.d. values for residues 13–47.
[b] r.m.s.d. values for residues in secondary structures (27–29, 37–47).

RESULTS AND DISCUSSION

Structure of ZBD Monomeric Subunit—The structure of ZBD was solved based on 565 intramolecular NOE observations and data base derived torsion angle restraints (Table I). Resonances from the first ten residues and the last two residues of ZBD were either unobservable or unassignable indicating that these regions were largely unstructured (Figs. 1 and 2). Measurements of the amide heteronuclear ^{1}H-^{15}N NOEs, which are sensitive to bond motions occurring faster than overall rotational correlation time of the molecule, indicate that the folded ZBD core spans residues Leu^{11}–Arg^{48} (Fig. 1). The core of ZBD is organized into two hairpins (Tyr^{13} to Ser^{20}; Lys^{26} to Ser^{36}) followed by one α-helix (D37 to I46). No long range (i, $i + 4$) NOEs were observed from Arg^{48} to His^{57}.

Each monomer has a fold resembling that of the treble clef zinc finger family (43). This family of metal-binding proteins is distinct from other zinc finger folds (44) and includes the NH_2-terminal zinc finger of GATA-1, FYVE domains, the transcription factor TFIIIH p44 subunit, and the zinc binding domains of RING proteins. Although ZBD and the NH_2-terminal DNA binding domain of GATA-1 (45), for example, have little sequence similarity, they share a similar secondary structure (Fig. 1), illustrating the diversity of this motif. Treble clef zinc fingers are characterized by two β-hairpins and one α-helix. Among members of the treble clef zinc finger family, a Zn(II) ion is coordinated by two residues in the first β-hairpin, one residue in the second β-hairpin and one residues in the NH_2 terminus of the α-helix. In ZBD, four cysteines (Cys^{14}, Cys^{17},

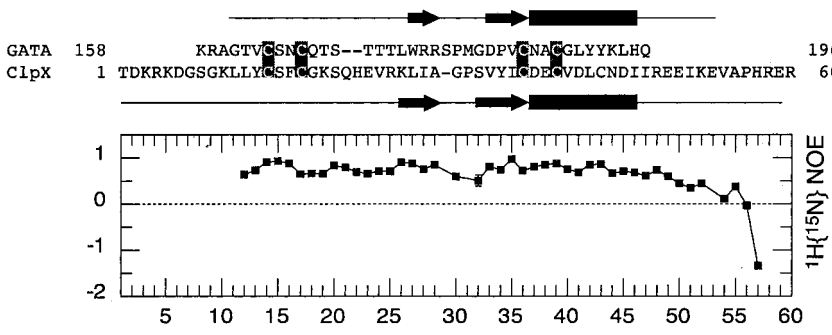

FIG. 1. **Secondary structure of ZBD.** Primary and secondary structure alignment of ZBD from ClpX with the NH_2-terminal zinc finger from chicken GATA-1 DNA binding domain (Protein Data Bank code 1GAT). Cysteines involved in Zn(II) coordination are highlighted. The plot of ^{1}H{^{15}N} amide heteronuclear NOE values is shown below the alignment.

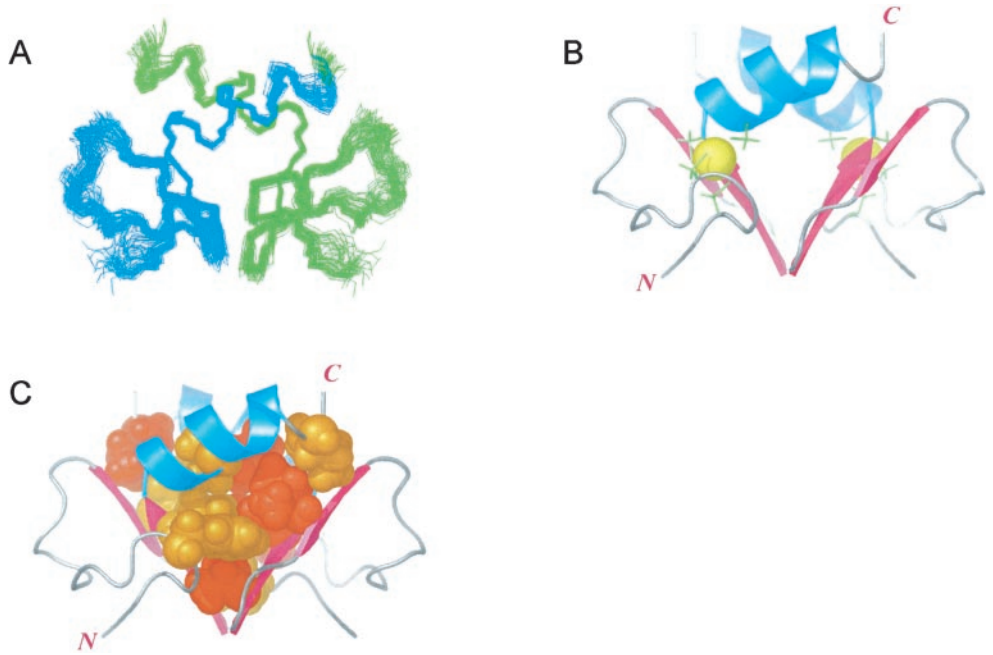

FIG. 2. **Structure of ZBD.** *A*, backbone superposition of 25 low energy structures of the ZBD homodimer. *B*, ribbon representation of the lowest energy structure. Helices are colored *blue*, and strands are colored *red*. Zn(II) atoms are shown as *yellow spheres*, and the cysteines involved in chelating the Zn(II) are drawn as *yellow sticks*. *C*, hydrophobic residues forming the core of the ZBD dimer are shown as space-filling models. These residues are Phe[16], Ile[28], Val[33], Ile[35], Val[40], and Ile[47]. Residues from the left monomer are colored *orange*, while those from the right monomer are colored *red*.

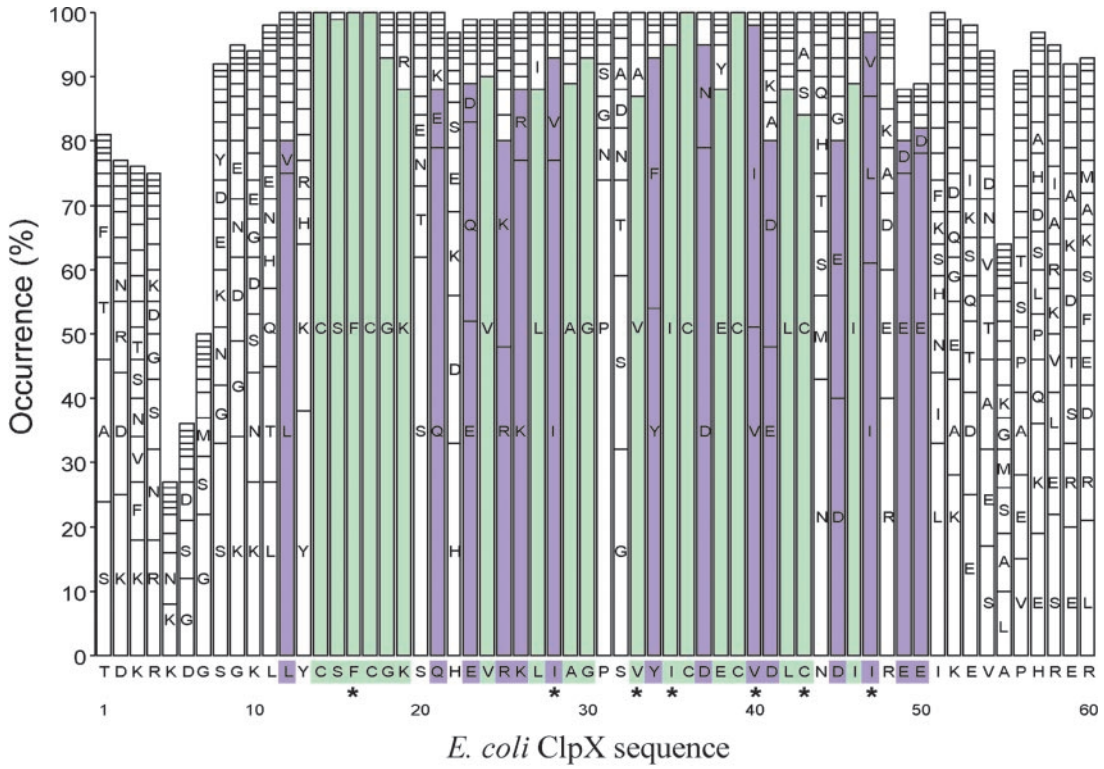

FIG. 3. **Sequence conservation of ZBD.** Sequences from 100 different bacteria were aligned using ClustalW. Residues that are identical in >80% of the sequences are *shaded* in *green*, while residues that are similar in >80% of the sequences (according to Blosum62 matrix) are *shaded violet*. Residue numbering is according to *E. coli* ClpX protein. *Bars* less than 100% are due to a lack of residues at the corresponding positions in some bacteria. Residues whose side chains are buried in the ZBD dimer interface are indicated by an *asterisk*.

Cys[36], and Cys[39]) are involved in the coordination of one Zn(II) ion per monomer (31, 46). Despite that only six residues are similar between the treble clef zinc fingers of ClpX and chicken GATA-1, with four of these residues being the coordinating cysteines, the C^{α} atoms of ZBD and GATA-1 (Protein Data Bank code 1GAT) superimpose with an r.m.s.d. of 1.9 Å. On the other hand, according to CE (47) and DALI (48) search engines using a 3-Å similarity threshold, the ZBD dimer is not related to any protein fold that has been described to date.

The Dimer Interface—The ZBD dimer (Fig. 2) is defined by 47 intermolecular NOEs originating predominantly from a hydrophobic cluster consisting of Phe[16], Ile[28], Val[33], Ile[35], Val[40],

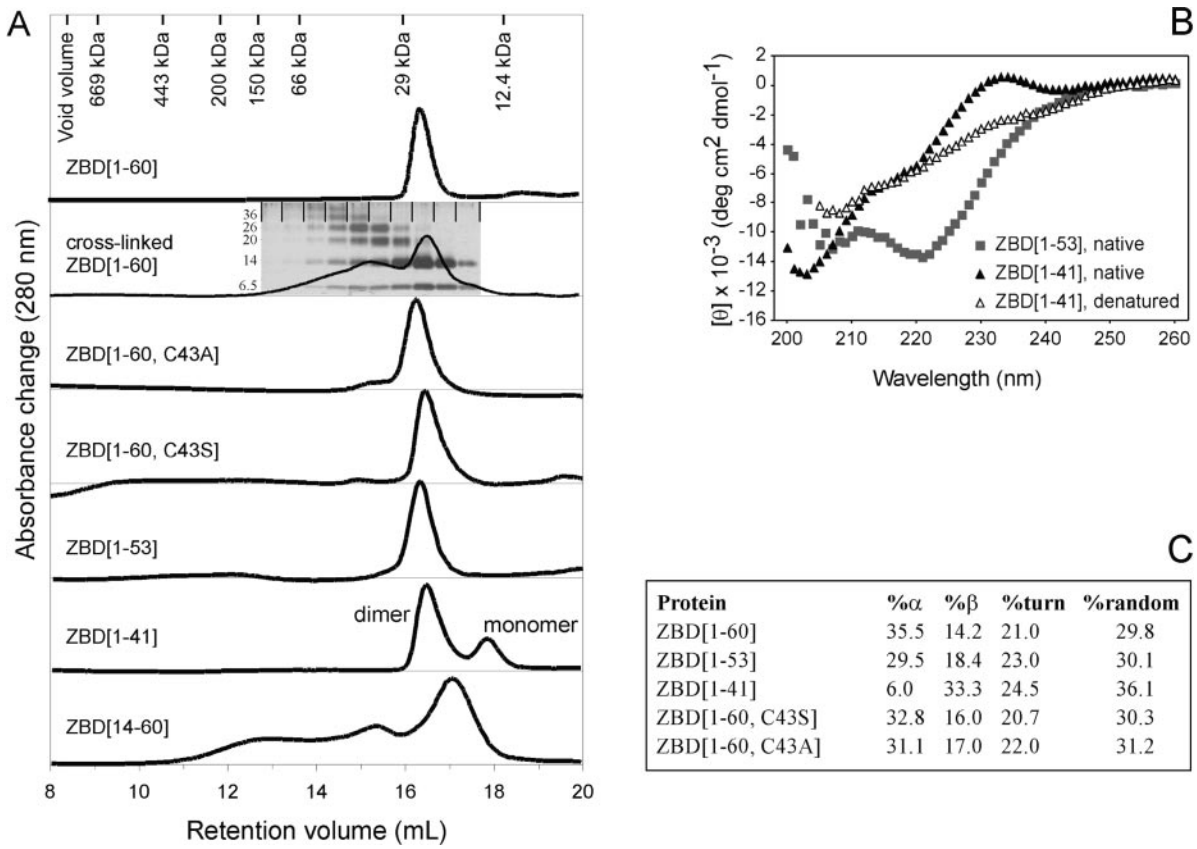

C

Protein	%α	%β	%turn	%random
ZBD[1-60]	35.5	14.2	21.0	29.8
ZBD[1-53]	29.5	18.4	23.0	30.1
ZBD[1-41]	6.0	33.3	24.5	36.1
ZBD[1-60, C43S]	32.8	16.0	20.7	30.3
ZBD[1-60, C43A]	31.1	17.0	22.0	31.2

FIG. 4. **Analysis of the ZBD dimer interface.** *A*, the oligomeric states of ZBD-(1–60) and of ZBD mutants were analyzed by size exclusion chromatography on a Superdex 200 HR 10/30 column equilibrated with 25 mM Tris-HCl, pH 8, 150 mM NaCl, and 1 mM dithiothreitol. Absorbance was monitored at 280 nm. Molecular mass standards are shown along the top. For cross-linked ZBD-(1–60), *second panel* from *top*, ZBD-(1–60) was incubated at 30 μM with 0.05% glutaraldehyde for 15 min. The sample was then separated on the gel filtration column, and 500-μl fractions were collected and analyzed by SDS-PAGE and silver-stained. The positions of the molecular mass standards are shown on the gel. In addition to the cross-linked ZBD dimers, higher order nonspecific cross-linked oligomers are observed at this concentration. *B*, CD spectra, expressed as mean residue ellipticity, of native ZBD-(1–53) (■) and of native ZBD-(1–41) (▲) at 10 °C, and of the denatured ZBD-(1–41) (△) at 110 °C, are shown. The spectrum of denatured ZBD-(1–53) is similar to that of denatured ZBD-(1–41) and is not shown. Proteins were at a concentration of 30 μM in the buffer listed above. *C*, CD spectra of different ZBD constructs were analyzed for secondary structure content using CDPro (lamar.colostate.edu/~sreeram/CDPro/main.html). The average values are listed.

Cys^{43}, and Ile^{47} (Fig. 2*C*). From an alignment of 100 bacterial ClpX NH_2-terminal sequences (Fig. 3), this hydrophobic cluster is well conserved suggesting a strong evolutionary pressure to maintain the dimeric form. In contrast, monomeric chicken GATA-1 does not possess these sequence signatures (Fig. 1).

As calculated by MOLMOL (40) each monomer has a solvent accessible surface area of 3242 Å and contributes 945 $Å^2$ to the dimer interface. Dimerization brings the sole α-helices from each monomer together in an anti-parallel orientation when viewed from one symmetry axis, and the second β-hairpins (Fig. 1) together along a second symmetry axis (Fig. 2). The nature and extent of the interface explain why the ZBD dimer is very stable (ΔG_U = 9.9 kcal/mol at 25 °C) and does not dissociate into monomers even at 1 μM concentrations (31).

To further characterize the sequence elements involved in the dimer interface, ZBD-(1–60) (residues 1–60) and different truncations of ZBD were analyzed by size exclusion chromatography. ZBD-(1–60) migrated as a dimer in a single peak as determined by cross-linking: cross-linked ZBD-(1–60) migrated mainly at the same position as the non-cross-linked sample (*second panel* from *top* in Fig. 4*A*). Mutating Cys^{43} to alanine or serine did not affect the migration pattern of ZBD-(1–60), indicating that this fifth cysteine in the ClpX sequence is not involved in the dimerization of ZBD. Removal of residues 1–13 preceding the first cysteine or residues 54–60 after the α-helix also did not affect ZBD dimerization. ZBD-(14–60) was not very stable and had a tendency to aggregate in a time-dependent manner, while ZBD-(1–53) represents the fragment identified by Singh *et al.* (22). Only the truncation of the α-helix, represented by ZBD-(1–41), weakened the affinity between the monomers and as a result both monomers and dimers could be detected (*second panel* from *bottom* in Fig. 4*A*).

The results of the size exclusion chromatography were further substantiated by CD scans of the different truncation mutants (Fig. 4, *B* and *C*). Analysis of the CD spectra of all the mutants examined indicated that their secondary structure content were similar to that of ZBD-(1–60) except for ZBD-(1–41), which had little α-helical content and increased β content (Fig. 4*C*) as expected from the structure (Fig. 2).

Evolutionary Aspects of the ZBD Structure—ClpA and ClpB are two other members of the Clp/Hsp100 family of proteins in *E. coli*. ClpA and ClpB have an NH_2-terminal domain of about 140–150 residues followed by two ATPase domains (49). ClpA proteins, which lack the NH_2-terminal domain, can mediate the ClpP dependent degradation of SsrA-tagged substrates (22, 24, 25) but not of other substrates such as RepA (24). The NH_2 terminus of ClpA is also important for cofactor binding such as ClpS (25). On the other hand, ClpB lacking its NH_2 terminus was shown to be either inactive or active as a chaperone *in vitro* depending on the assay being used (26).

The structures of the ClpA and ClpB NH_2-terminal domains have been solved by x-ray crystallographic methods (30, 50, 51). The structures of the two domains reveal two four-helix tandem repeats, about 70 residues in length, with pseudo 2-fold

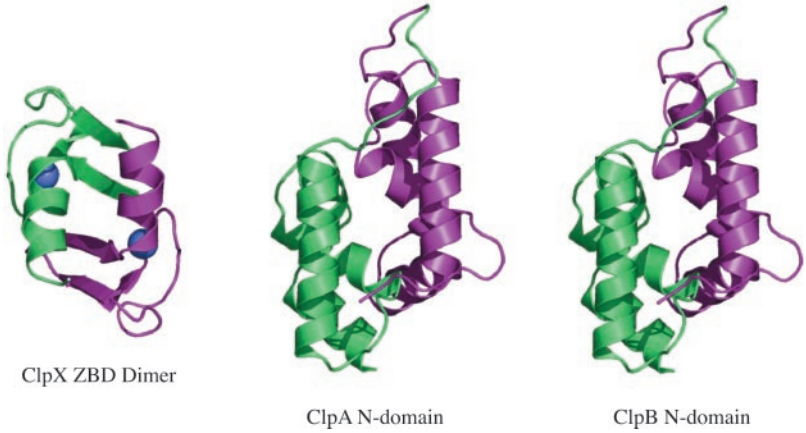

FIG. 5. **Comparison of the NH_2-terminal domains of ClpX, ClpA, and ClpB.** Structures of the ZBD dimer, ClpA N-domain (Protein Data Bank code 1K6K) (30), and ClpB N-domain (Protein Data Bank code 1KHY) (51) are shown. Zn(II) atoms are drawn as *spheres*.

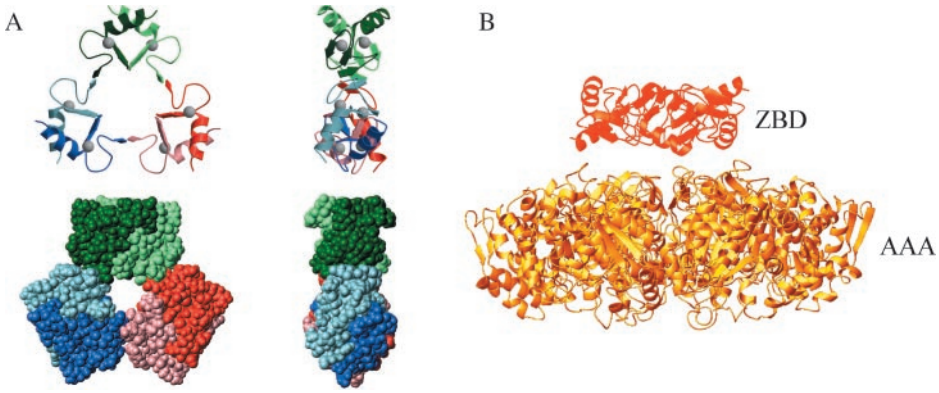

FIG. 6. **The trimer-of-dimers model of ZBD.** *A*, ribbon and space-filling representation of the trimer-of-dimers model of ZBD. *B*, ribbon representation of the trimer-of-dimers model of ZBD shown on *top* of the AAA hexamer model of ClpX constructed based on the HslU hexameric structure (54) using Swiss-Model (59).

symmetry. Despite the lack of sequence and secondary structure conservation, the ClpX ZBD dimer and the NH_2-terminal domains of ClpA and ClpB have a similar overall general topology (Fig. 5).

The dimerization of the NH_2 terminus of ClpX and the formation of a pseudodimer by the NH_2-terminal domains of ClpA and ClpB may have been the result of a series of convergent evolutionary events. In ClpX, dimerization is facilitated by the self-association of the treble clef zinger motifs from two separate molecules, while the formation of the pseudo dimer by the NH_2-terminal domains of ClpA and ClpB is promoted by a tandemly repeated motif. Alternatively, if a divergent evolutionary relationship is assumed to exist among the ClpX ZBD and the NH_2-terminal domains of ClpA and ClpB, it presupposes a common structural ancestor. In this scenario, a *clpX*-like gene would have inserted itself into another *clpX*-like gene at a location corresponding to the linker region between ZBD and the AAA domains. This has also been proposed by Guo *et al.* (30, 52). Following this view, two similarly positioned antiparallel α-helices in the ClpX ZBD dimer and in the NH_2-terminal pseudodimer of ClpA and ClpB (the helices facing the reader in Fig. 5) could be considered a vestigal element of a distantly related progenitor. It is intriguing to note that the NH_2-terminal domain of ClpA has the rudiments of zinc binding via two histidines, one glutamic acid, and a water molecule (52) rather than four cysteines as in the case of ClpX. In any case, it is important to emphasize that there is no strutural similarity between the ClpX ZBD dimer and the NH_2-terminal domains of ClpA and ClpB.

The Trimer-of-Dimers Model of ZBD—Electron microscopy studies demonstrate that the ClpX ATPase domain forms hexamers in the presence or absence of ZBD (22, 27). As the ZBD forms dimers when segregated from ClpX, the ClpX hexamer may be considered as a trimer-of-dimers. When ZBD is viewed in an orientation shown in Fig. 2, there is an element of 3-fold symmetry where the second β-hairpins cross. Building on this observation, a simple 3-fold rotation of the dimer produces a ring-like model whose subunits complement each other well (Fig. 6*A*). Although this model is purely speculative, arrangement of three ClpX ZBD dimers in this manner produces a structure that agrees with the structural and functional organization expected for the ClpXP complex. This model satisfies the 3-fold symmetry of the structure, creates a ring structure that is consistent with the other parts of ClpX and with ClpP, and minimizes steric clashes.

When the ZBD trimer-of-dimers model is viewed from the side of the ring, a second 3-fold symmetry element is apparent. This element is composed of three two-stranded anti-parallel β sheets. Two of the β sheets are derived from each of the monomers in the ZBD dimer, while the third β sheet is created from an intermolecular interaction between residues Leu^{11}–Tyr^{13} of adjacent dimers. In the dimeric ZBD structure, residues Leu^{11}–Tyr^{13} are deemed to be in an extended conformation as evidenced by relatively lower $^1H\{^{15}N\}$ heteronuclear NOE values; however, backbone chemical shift analysis suggests that they form a short β-strand. In light of the proposed hexameric model, a degree of conformational freedom in Leu^{11}–Tyr^{13} would facilitate the interaction of β-strands from two adjacent ZBD dimers. As can be seen from the space-filling representation of the hexameric model (Fig. 6*A*), much of the possible interdimer interactions are localized to this region. We further speculate that the entropic cost of ordering Leu^{11}–Tyr^{13} might reduce the possibility of formation of the hexameric state until further stabilizing conditions such as substrate binding are met.

The space-filling model of the ZBD trimer-of-dimers also highlights a central pore of about 14 Å in diameter. The residues that comprise the pore in this model are predominantly hydrophobic. If the ClpX ATPase domain is modeled on the solved structure of the HslU ATPase domain (53–55), then the

pore lined by the GYVG sequence motif has an approximate diameter of 25 Å. The outer diameter of the ZBD hexamer is 60 Å or approximately half the distance of the modeled ATPase domain (Fig. 6*B*). From Arg^{48}, the last structured residue observed in the ZBD dimer, to Ala^{62}, which represents the modeled NH_2-terminal boundary of the AAA domain, a 14-residue linker remains. If this linker is extended in the ClpX hexamer, three ZBD dimers are afforded a considerable degree of flexibility, assuming 3.6 Å per residue (56). Mechanistically, such conformational freedom would allow the ZBD dimers to reach out from the ATPase ring toward a substrate protein.

The trimer-of-dimers model of ZBD may represent a closed conformation of ClpX. We speculate that in this state, an unfolded substrate protein would be trapped underneath the ZBD lid forcing the substrate to be translocated into the ClpP chamber. The sequence of events producing movement of the ZBD to form the closed conformation likely requires ATP binding and/or hydrolysis in the ATPase domain of ClpX. Since it has been shown that ZBD has low affinity to the rest of ClpX (22), the linker between ZBD and the AAA domain might play a major role in communicating the conformational changes between these two domains. If the trimer-of-dimers model of ZBD (Fig. 6*A*) represents the closed conformation of ClpX, then it follows that an open conformation of the chaperone exists where the dimers are apart ready to capture an incoming substrate protein or to bind a cofactor. Experiments are under way to test these hypotheses.

Zinc fingers in proteins that interact with DNA or RNA are among the best studied domains, but, more recently, it is becoming clear that zinc fingers can also mediate protein-protein interactions (57). Furthermore, there are several known cases of zinc fingers that form homo- or heterodimers (58). The ClpX ZBD dimer represents another such case. The structure of the ClpX ZBD provides insight as to how chaperones with multiple AAA domains, such as ClpA and ClpB, are guided evolutionarily toward a common function. Furthermore, the structure also sheds some light on the possible conformational changes that ClpX might undergo during its functional cycle.

Acknowledgments—We are grateful to Lewis Kay and Ranjith Muhandiram (University of Toronto) for assistance with NMR data collection. Members of the Donaldson laboratory (H. Chasiotis, J. Kwan, and A. Maida) and the Houry laboratory (J. Snider, T. Davidson, and G. Thibault) provided technical support and helpful comments throughout the preparation of this manuscript.

REFERENCES

1. Hartl, F. U., and Hayer-Hartl, M. (2002) *Science* **295,** 1852–1858
2. Gottesman, S., Clark, W. P., de Crecy-Lagard, V., and Maurizi, M. R. (1993) *J. Biol. Chem.* **268,** 22618–22626
3. Wojtkowiak, D., Georgopoulos, C., and Zylicz, M. (1993) *J. Biol. Chem.* **268,** 22609–22617
4. Schirmer, E. C., Glover, J. R., Singer, M. A., and Lindquist, S. (1996) *Trends Biochem. Sci.* **21,** 289–296
5. Beuron, F., Maurizi, M. R., Belnap, D. M., Kocsis, E., Booy, F. P., Kessel, M., and Steven, A. C. (1998) *J. Struct. Biol.* **123,** 248–259
6. Schmidt, M., Lupas, A. N., and Finley, D. (1999) *Curr. Opin. Chem. Biol.* **3,** 584–591
7. Kessel, M., Maurizi, M. R., Kim, B., Kocsis, E., Trus, B. L., Singh, S. K., and Steven, A. C. (1995) *J. Mol. Biol.* **250,** 587–594
8. Grimaud, R., Kessel, M., Beuron, F., Steven, A. C., and Maurizi, M. R. (1998) *J. Biol. Chem.* **273,** 12476–12481
9. Levchenko, I., Luo, L., and Baker, T. A. (1995) *Genes Dev.* **9,** 2399–2408
10. Jones, J. M., Welty, D. J., and Nakai, H. (1998) *J. Biol. Chem.* **273,** 459–465
11. Gonciarz-Swiatek, M., Wawrzynow, A., Um, S. J., Learn, B. A., McMacken, R., Kelley, W. L., Georgopoulos, C., Sliekers, O., and Zylicz, M. (1999) *J. Biol. Chem.* **274,** 13999–14005
12. Gonzalez, M., Rasulova, F., Maurizi, M. R., and Woodgate, R. (2000) *EMBO J.* **19,** 5251–5258
13. Neher, S. B., Flynn, J. M., Sauer, R. T., and Baker, T. A. (2003) *Genes Dev.* **17,** 1084–1089
14. Flynn, J. M., Neher, S. B., Kim, Y. I., Sauer, R. T., and Baker, T. A. (2003) *Mol. Cell* **11,** 671–683
15. Tu, G. F., Reid, G. E., Zhang, J. G., Moritz, R. L., and Simpson, R. J. (1995) *J. Biol. Chem.* **270,** 9322–9326
16. Keiler, K. C., Waller, P. R., and Sauer, R. T. (1996) *Science* **271,** 990–993
17. Gottesman, S., Roche, E., Zhou, Y., and Sauer, R. T. (1998) *Genes Dev.* **12,** 1338–1347
18. Levchenko, I., Seidel, M., Sauer, R. T., and Baker, T. A. (2000) *Science* **289,** 2354–2356
19. Wah, D. A., Levchenko, I., Baker, T. A., and Sauer, R. T. (2002) *Chem. Biol.* **9,** 1237–1245
20. Zhou, Y., Gottesman, S., Hoskins, J. R., Maurizi, M. R., and Wickner, S. (2001) *Genes Dev.* **15,** 627–637
21. Neuwald, A. F., Aravind, L., Spouge, J. L., and Koonin, E. V. (1999) *Genome Res.* **9,** 27–43
22. Singh, S. K., Rozycki, J., Ortega, J., Ishikawa, T., Lo, J., Steven, A. C., and Maurizi, M. R. (2001) *J. Biol. Chem.* **276,** 29420–29429
23. Dougan, D., Mogk, A., Zeth, K., Turgay, K., and Bukau, B. (2002) *FEBS Lett.* **529,** 6–10
24. Lo, J. H., Baker, T. A., and Sauer, R. T. (2001) *Protein Sci.* **10,** 551–559
25. Dougan, D. A., Reid, B. G., Horwich, A. L., and Bukau, B. (2002) *Mol. Cell* **9,** 673–683
26. Barnett, M. E., Zolkiewska, A., and Zolkiewski, M. (2000) *J. Biol. Chem.* **275,** 37565–37571
27. Ortega, J., Singh, S. K., Ishikawa, T., Maurizi, M. R., and Steven, A. C. (2000) *Mol. Cell* **6,** 1515–1521
28. Reid, B. G., Fenton, W. A., Horwich, A. L., and Weber-Ban, E. U. (2001) *Proc. Natl. Acad. Sci. U. S. A.* **98,** 3768–3772
29. Kim, Y. I., Burton, R. E., Burton, B. M., Sauer, R. T., and Baker, T. A. (2000) *Mol. Cell* **5,** 639–648
30. Guo, F., Maurizi, M. R., Esser, L., and Xia, D. (2002) *J. Biol. Chem.* **277,** 46743–46752
31. Wojtyra, U., Thibault, G., Tuite, A., and Houry, W. A. (2003) *J. Biol. Chem.* **278,** 48981–48990
32. Cai, M., Huang, Y., Sakaguchi, K., Clore, G. M., Gronenborn, A. M., and Craigie, R. (1998) *J. Biomol. NMR* **11,** 97–102
33. Delaglio, F., Grzesiek, S., Vuister, G. W., Zhu, G., Pfeifer, J., and Bax, A. (1995) *J. Biomol. NMR* **6,** 277–293
34. Johnson, B. A., and Blevins, J. (1994) *J. Biomol. NMR* **4,** 603–614
35. Zwahlen, C., Legault, P., Vincent, S. J. F., Greenblatt, J., Konrat, R., and Kay, L. E. (1997) *J. Am. Chem. Soc.* **119,** 6711–6721
36. Cornilescu, G., Delaglio, F., and Bax, A. (1999) *J. Biomol. NMR* **13,** 289–302
37. Linge, J. P., O'Donoghue, S. I., and Nilges, M. (2001) *Methods Enzymol.* **339,** 71–90
38. Schwieters, C. D., Kuszewski, J. J., Tjandra, N., and Clore, G. M. (2003) *J. Magn. Res.* **160,** 66–74
39. Guex, N., and Peitsch, M. C. (1997) *Electrophoresis* **18,** 2714–2723
40. Koradi, R., Billeter, M., and Wuthrich, K. (1996) *J. Mol. Graph.* **14,** 29–32, 51–55
41. Kraulis, P. J. (1991) *J. Appl. Crystallogr.* **24,** 946–950
42. Merritt, E. A., and Bacon, D. J. (1997) *Methods Enzymol.* **277,** 505–524
43. Grishin, N. V. (2001) *Nucleic Acids Res.* **29,** 1703–1714
44. Krishna, S. S., Majumdar, I., and Grishin, N. V. (2003) *Nucleic Acids Res.* **31,** 532–550
45. Omichinski, J. G., Clore, G. M., Schaad, O., Felsenfeld, G., Trainor, C., Appella, E., Stahl, S. J., and Gronenborn, A. M. (1993) *Science* **261,** 438–446
46. Banecki, B., Wawrzynow, A., Puzewicz, J., Georgopoulos, C., and Zylicz, M. (2001) *J. Biol. Chem.* **276,** 18843–18848
47. Shindyalov, I. N., and Bourne, P. E. (1988) *Protein Eng.* **11,** 739–747
48. Holm, L., and Sander, C. (1993) *J. Mol. Biol.* **233,** 123–138
49. Hoskins, J. R., Sharma, S., Sathyanarayana, B. K., and Wickner, S. (2002) *Adv. Protein Chem.* **59,** 413–429
50. Zeth, K., Ravelli, R. B., Paal, K., Cusack, S., Bukau, B., and Dougan, D. A. (2002) *Nat. Struct. Biol.* **9,** 906–911
51. Li, J., and Sha, B. (2003) *Structure* (*Lond.*) **11,** 323–328
52. Guo, F., Esser, L., Singh, S. K., Maurizi, M. R., and Xia, D. (2002) *J. Biol. Chem.* **277,** 46753–46762
53. Bochtler, M., Hartmann, C., Song, H. K., Bourenkov, G. P., Bartunik, H. D., and Huber, R. (2000) *Nature* **403,** 800–805
54. Wang, J., Song, J. J., Franklin, M. C., Kamtekar, S., Im, Y. J., Rho, S. H., Seong, I. S., Lee, C. S., Chung, C. H., and Eom, S. H. (2001) *Structure* (*Lond.*) **9,** 177–184
55. Wang, J., Song, J. J., Seong, I. S., Franklin, M. C., Kamtekar, S., Eom, S. H., and Chung, C. H. (2001) *Structure* (*Lond.*) **9,** 1107–1116
56. Creighton, T. E. (1993) in *Proteins: Structures and Molecular Properties*, 2nd Ed., pp. 1–47, W. H. Freeman and Co., New York
57. Mackay, J. P., and Crossley, M. (1998) *Trends Biochem. Sci.* **23,** 1–4
58. McCarty, A. S., Kleiger, G., Eisenberg, D., and Smale, S. T. (2003) *Mol. Cell* **11,** 459–470
59. Peitsch, M. C. (1996) *Biochem. Soc. Trans.* **24,** 274–279